2011 American Control Conference
on O'Farrell Street, San Francisco, CA, USA
June 29 - July 01, 2011

Large Aperture Segmented Space Telescope (LASST): Can we control a 12 000 segment mirror?

Douglas G. MacMynowski and Mattias Björklund

Abstract— **The primary mirror diameter of affordable space telescopes is limited by mass and manufacturing cost. Currently planned optical/near-IR space telescopes use a segmented primary mirror with relatively few segments, and make limited use of real-time position control. However, control can be used as an enabler for a fundamentally different, very highly-segmented architecture, leading to a significant reduction in areal density, and hence a significant increase in the realistically achievable diameter of a space telescope. Small segments can be thinner, and overall mirror stiffness provided by control rather than a back-support structure. However, the resulting control problem involves thousands of actuators and sensors, and many lightly damped modes within the bandwidth. A local control approach similar to that previously developed for large deformable mirrors can provide robust performance for this problem. This is illustrated here for a 30 m diameter primary mirror composed of 12 000 0.3 m diameter segments. The areal density might be as low as 3–4 kg/m^2, nearly an order of magnitude lower than current designs.**

I. INTRODUCTION

While ground-based astronomy is less expensive, telescopes in space allow science in wavelength bands absorbed by Earth's atmosphere, avoid atmospheric distortion (which is never fully correctable by adaptive optics, particularly at visible wavelengths), provide a stable environment with low background, and permit long integration times [1].

A larger telescope aperture both collects more photons, and provides higher angular resolution (if not limited by observing through an atmosphere). Ground-based optical telescopes are currently being designed with segmented primary mirror diameters of 30 m (using 492 segments) [2] and 42 m (984 segments) [3]. In contrast, the 18-segment primary mirror of the IR-optimized James Webb Space Telescope (JWST) [4] to be launched in 2014 is 6.5 m, and future designs for the Advanced Technology Large Aperture Space Telescope (ATLAST) range from a monolithic 8 m mirror to segmented 9.2 and 16.8 m designs [1], all significantly smaller than what can be achieved at much lower cost on the ground. The goal herein is to propose active control of the mirror segments as a key enabler for building much larger diameter telescopes in space.

A key driver limiting affordable aperture sizes in space is the primary mirror mass or areal density, with the JWST and ATLAST segmented mirrors being of order 25 kg/m^2 (with additional mass of support structure behind them). In contrast, actuated hybrid silicon carbide mirror segments have been proposed with areal densities <10 kg/m^2 [5], as low as 3 kg/m^2 using 1 mm thick silicon segments [6], and potentially even thinner and lighter with internal actuation [7]. However, the highly segmented space telescope design presented in [6] (using $\sim$0.3 m diameter segments) did not include controls analysis, and the aim here is to illustrate that the resulting large numbers of segments (e.g. 12 000 for a 30 m mirror) can be robustly controlled with sufficient performance. (There are of course additional design and manufacturability issues regarding the segments, actuation, and sensing.) Highly-segmented concepts have also been introduced for ground-based telescopes [8]. Membrane-based approaches have also been suggested for large lightweight space telescopes (see e.g. the review by Santer and Seffen [9]), however, these may also require somewhat similar controls technology to provide adequate optical surface quality.

The total mass of the JWST telescope (not instrumentation or spacecraft bus) is roughly 4 times larger than the mass of the primary mirror, and thus it is insufficient to address only the areal density of the mirror and not also develop a strategy to minimize structural mass. Thus while some mechanical interface is required between neighboring segments to provide in-plane stiffness, providing a stiff back-support structure would defeat the purpose of minimizing mirror areal density. Minimizing structural mass results in a mirror that is highly flexible in its optically-relevant out-of-plane motion, and active surface control will be required: even though there are few disturbances in space, some stiffness is required to enable repointing of the telescope in reasonable time. Thus the control problem involves thousands of actuators and sensors, and thousands of lightly-damped structural modes within the control bandwidth. A solution for this problem has recently been proposed in the context of large (1-3 m) deformable mirrors for ground-based adaptive optics [10]. The first observation is that it is always possible to implement collocated rate feedback with some minimum but finite bandwidth (i.e., with real actuators and sensors). Second, collocated position control guarantees robustness but does not provide adequate stiffness for high spatial-frequency deformations, while feedback of global sensor information provides performance but poor robustness. The proposed strategy uses only local information to yield performance near that of a global solution, while retaining robustness by not relying on global information.

While the objective here is to demonstrate that a large array of segments can be controlled, and not to provide a detailed point design of a telescope using these ideas, a general description is useful for defining design constraints (section II). The remaining sections define the simulation, and describe the control.

D. G. MacMynowski is in the Department of Control and Dynamical Systems, California Institute of Technology, Pasadena, CA 91125. macmardg@cds.caltech.edu

M. Björklund is at KTH, Stockholm, Sweden.

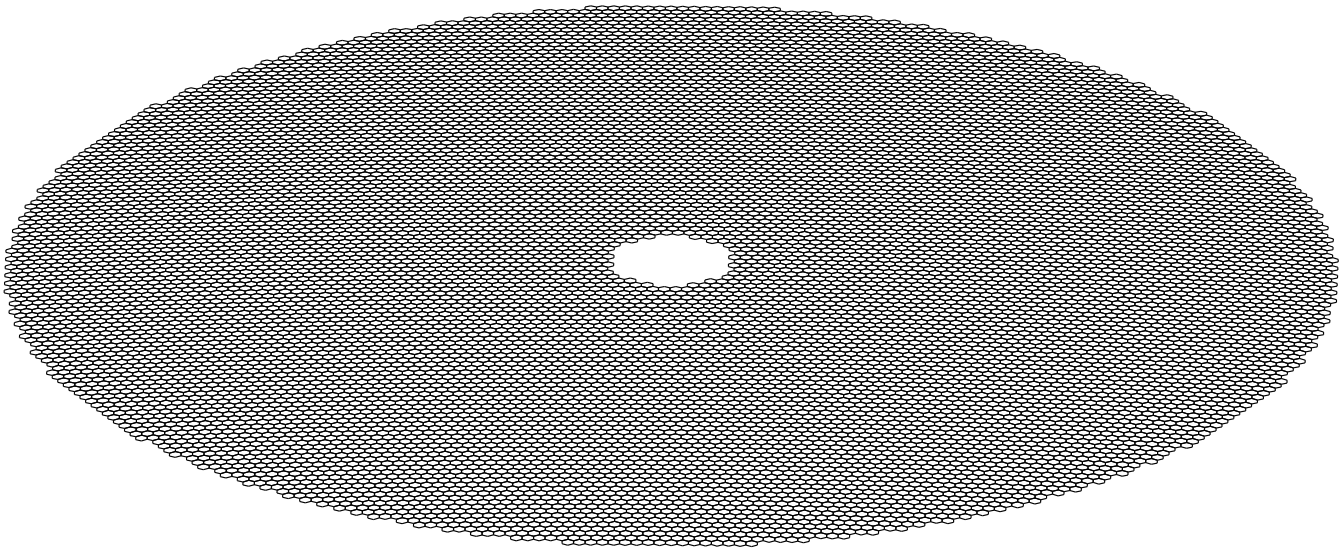

Fig. 1. Schematic of a 12 000 segment mirror (viewed from a 30° elevation angle), with hexagonal segment diameter 1% of the mirror diameter (e.g., 30 m with 0.3 m segments). The secondary mirror would be on a separate formation-flying spacecraft.

II. CONCEPT

Science cases for future large-aperture optical and near-IR space telescopes are described, for example, in [1]. One motivator for such a facility would be the capability for assessing the potential for life on Earth-like planets of other stars. The larger the aperture, the greater number of star systems can be considered, both because more light-gathering capability means less integration time, and because higher resolution allows distinguishing star-light from planet at greater distances from the Earth. For this type of science, the overall field-of-view would not need to be very large. Sufficient integration time is required for spectroscopic measurements to understand atmospheric composition, while the total number of targets to be evaluated by the facility during its lifetime might be only a few thousand; for this type of mission, then, it may be acceptable if it takes many hours to change the orientation of the telescope to point at a different target. However, a settling time of days before acquiring a new target would significantly impact the science mission. For the simulation parameters described in the next section, the first resonant frequency of a 30 m primary mirror is ~ 0.1 Hz; with damping as low as 0.1%, the uncontrolled settling time to a few nm residual error from a 90° degree slew maneouver would be of order a day.

The key innovation herein is thus a strategy that enables control of a highly-segmented filled-aperture primary mirror. An example is illustrated in Fig. 1, with $N = 12\,000$ hexagonal segments with maximum radius 0.15 m (as in [6]). Mass is minimized both by (i) reducing segment size so that segment thickness can be reduced, without requiring additional degrees of freedom of actuation internal to the segment for shape control, and (ii) minimizing the mechanical interconnections between segments. In-space assembly, either robotic or with astronauts, is plausible if the interconnection tasks are straightforward, and if control can be used to correct errors resulting from not having a precision deployable structure [5].

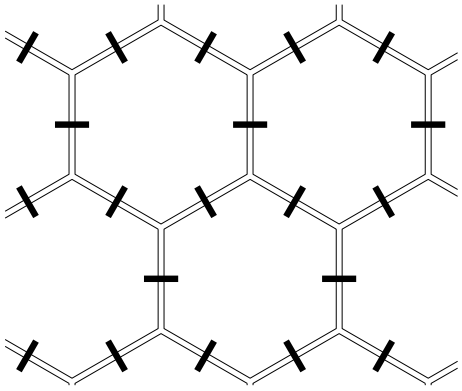

Fig. 2. Detail on segmentation geometry (with gaps enlarged for clarity), and using a single mechanical interconnection between neighbouring segments. The interconnection must be lightweight and designed for ease of assembly. Its primary purpose is to provide in-plane stiffness, but it will also provide some stiffness to both relative out-of-plane segment motion and relative dihedral angle change between segments. Two degrees of freedom of actuation provide both relative force and torque.

The mechanical interface between neighbouring segments provides stiffness for the in-plane degrees of freedom of the segment array, but does not need to provide significant stiffness for the out-of-plane degrees of freedom, since these will need to be actively controlled. A single interface between segments, as shown in Fig. 2, simplifies assembly, but requires that the interface provide stiffness and actuation authority for both relative out-of-plane inter-segment motion and inter-segment dihedral angle. (Note that with only a single degree of freedom per inter-segment edge, there would not be enough actuators to constrain the $3N$ degrees of freedom of the full segment array; with two degrees of freedom per edge there are more actuators than required to control segment rigid-body motion.) It is also possible to use two interconnects as pictured in [6]; the relative advantages are unclear without more detail design, but the

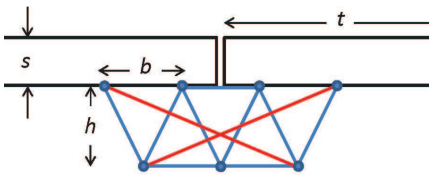

Fig. 3. Sketch of mechanical interconnect between neighboring segments used only to estimate representative stiffness values in simulation. The long diagonals (red) are active members to apply differential force/torques between segments; the truss provides differential translational and rotational stiffness between neighboring segments. The dimensions are chosen so that the interconnect structure could be folded behind a segment during launch.

basic control problem is the same, and we have chosen the single interconnect approach for simulations herein. Clearly, the design of the interconnection for both assembly and actuation is required; nominal parameters for stiffness are chosen based on the sketch in Fig. 3.

In addition to eliminating the structural weight supporting the primary mirror (M1), there is no need for structure between the primary and secondary mirror (M2) if formation flying is used for the M2 subsystem, as suggested in [6, 11] (and plausible if repointing of the telescope is not frequent). This also means that the primary focal-length of the telescope is not driven by structural weight or launch-packaging considerations, but only by the optical design; [11] proposes a focal-ratio of 20 so that for a 30 m primary mirror, M2 would be 0.6 km away. A consequence of long focal lengths and many segments is that the segment surface can be spherical rather than hyperbolic, and hence the segments can be identical; this is essential for minimizing manufacturing cost and also enables plausible in-space assembly rather than deployment. The overall M1 shape may still be parabolic or hyperbolic, and optical distortion may be improved with the ability to statically adjust the radius of curvature of each segment; the required adjustment decreases as the segment size decreases. As in [11], sun-shades can also be separate satellites flown in formation. Formation flying requires that the telescope not be in Earth orbit with its gravity-gradient torques, but at one of the stable Lagrange points (as JWST).

The mass of the spacecraft bus and instrumentation, located in the central obscuration of the primary mirror, will be significant, but does not scale with collecting area.

III. SIMULATION

Since the in-plane segment motions are passively constrained by the mechanical interconnection, only the three out-of-plane degrees of freedom need to be included in the dynamic model; here we describe the motion using segment piston (z) and rotations (Fig. 4) so $x_i = \begin{bmatrix}\phi_i & \theta_i & z_i\end{bmatrix}^T$, and the overall state vector is $x = \begin{bmatrix}x_1^T \cdots x_N^T\end{bmatrix}^T$ satisfying

$$M\ddot{x} + D\dot{x} + Kx = \Phi F$$

The notation $j = i(k)$ below refers to the segment j which borders segment i at orientation k.

The mechanical interconnection between two segments will create stiffness and actuator forces. For ease of calculation, an extra coordinate system (τ) (Fig. 4) is introduced

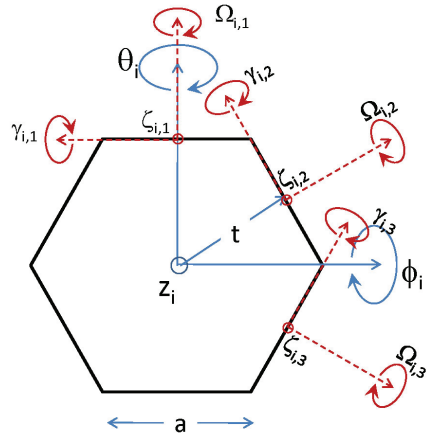

Fig. 4. Segment coordinate system z_i, θ_i, ϕ_i and rotated coordinate systems $\zeta_{i,k}$, $\gamma_{i,k}$, $\Omega_{i,k}$ (red) at the interface point with the neighbouring segment in the k^{th} direction. a is the segment radius or side length, $t = a\sqrt{3}/2$ is the radius at the interconnection points. Actuators at 3 of the 6 interconnection points are numbered with that segment, and the other 3 with the relevant neighbour.

for each connection point:

$$\tau_{i,k} = \begin{pmatrix} \Omega_{i,k} \\ \gamma_{i,k} \\ \zeta_{i,k} \end{pmatrix} = R_k x_i$$

where

$$R_k = \begin{pmatrix} \sin\left(\frac{\pi}{3}(k-1)\right) & \cos\left(\frac{\pi}{3}(k-1)\right) & 0 \\ -\cos\left(\frac{\pi}{3}(k-1)\right) & \sin\left(\frac{\pi}{3}(k-1)\right) & 0 \\ t\cos\left(\frac{\pi}{3}(k-1)\right) & -t\sin\left(\frac{\pi}{3}(k-1)\right) & 1 \end{pmatrix}$$

The stiffness and damping forces created in the connection joints will influence all three of its local τ coordinates, although the contribution in the Ω direction will be weak and could be ignored. Sufficient actuation degrees of freedom require only a force, F, and torque, M, corresponding to directions ζ and γ.

Neglecting damping, the equations of motion for each segment can then be written as

$$M_s\ddot{x}_i + \sum_{k=1}^{6} R_k^T K_s \left(\begin{pmatrix} \Omega_{\mathrm{i,k}} \\ \gamma_{i,k} \\ \zeta_{i,k} \end{pmatrix} + \begin{pmatrix} \Omega_{i(k),\mathrm{k+3}} \\ \gamma_{i(k),k+3} \\ -\zeta_{i(k),k+3} \end{pmatrix} \right)$$
$$= \sum_{k=1,3,5} K_{FX} \begin{pmatrix} F_{i,k} \\ M_{i,k} \end{pmatrix} + \sum_{k=2,4,6} K_{FX} \begin{pmatrix} -F_{i(k),k} \\ M_{i(k),k} \end{pmatrix} \quad (1)$$

where the relevant stiffness and actuation contributions are not included at boundary segments, and

$$M_s = \begin{pmatrix} J_\phi & 0 & 0 \\ 0 & J_\theta & 0 \\ 0 & 0 & m_s \end{pmatrix}$$

$$K_s = \begin{pmatrix} K_\Omega & 0 & 0 \\ 0 & K_\gamma & 0 \\ 0 & 0 & K_\zeta \end{pmatrix}$$

$$K_{FX} = \begin{pmatrix} t\cos\left(\frac{\pi}{3}(k-1)\right) & -\cos\left(\frac{\pi}{3}(k-1)\right) \\ -t\sin\left(\frac{\pi}{3}(k-1)\right) & \sin\left(\frac{\pi}{3}(k-1)\right) \\ 1 & 0 \end{pmatrix}$$

Damping $D = c_1 M + c_2 K$ is added, with c_1 and c_2 chosen to give 0.1% damping at the first resonance and at 500 Hz.

Parameter	Value	Parameter	Value
ρ	$2.95\times10^3\,\mathrm{kg/m^3}$	K_Ω	10
a	0.15 m	K_γ	4.2e3 Nm/rad
s	1 mm	K_ζ	3.7e6 N/m
b	0.04 m	M_{center}	4000 kg
N	12000	J_{center}	$3100\,\mathrm{kg\,m^2}$

TABLE I
PARAMETERS USED IN SIMULATION.

The spacecraft bus and instrumentation in the center of the mirror will have significant mass M_{center}. This mass is simulated by creating artificial rigidly-fused segments within the central obscuration with appropriate mass, so the bus is connected to the neighbouring segments with the same mechanical interconnection as between any other segments.

For the purposes of illustrating the control concept, we choose silicon carbide segments, $s = 1\,\mathrm{mm}$ thick with maximum radius $a = 15\,\mathrm{cm}$. The segment mass and moment of inertia is

$$m = \frac{3\sqrt{3}}{2}\rho s a^2 \qquad J_\theta = J\phi = \frac{5\sqrt{3}}{16}\rho s a^4$$

where ρ is the density; for analysis we assume that the optical coating, mechanical interconnections, actuators, sensors, and electronics/cabling will increase the $2.95\,\mathrm{kg/m^2}$ of the SiC alone by 50% without altering the mass distribution.

Representative values for the stiffness are obtained by analyzing the truss structure in Fig. 3; this is only to obtain reasonable parameter estimates and not to propose a specific design. The mass of each mechanical interconnect is assumed to be 10% of the mass of the SiC segment (so the total mechanical mass adds 30% to the mass). The depth influences the stiffness; this is chosen to be a fraction of the segment radius to allow a design that folds into the back of the segment for launch. This yields the parameters in Table I.

Using these parameters, the first resonance of a segment will be of order a kHz; above this frequency the simulation will not be accurate. For the purpose of understanding the low spatial/temporal frequency modes of the overall mirror, the flexibility of an individual segment can be ignored.

IV. CONTROL

A. Control problem

There are $3N$ controlled degrees of freedom for the overall segmented-mirror (the in-plane degrees of freedom are passively controlled by the mechanical interconnection), and slightly less than $6N$ degrees of freedom of relative actuation. The extra degrees of freedom could either be constrained to be zero, or used to provide small deformations of the segments to modify their radius of curvature in both the radial and azimuthal directions.

Two sensors are also needed on each edge to measure the relative motion between segments. A similar approach has been proven on ground-based segmented-mirror telescopes, with resolution of a few nm using either differential capacitive or differential inductive sensors. Unless a manufacturing approach is used that ensures sensor installation errors of nm, an initial phasing approach using starlight would be needed after the mirror was assembled in order to determine

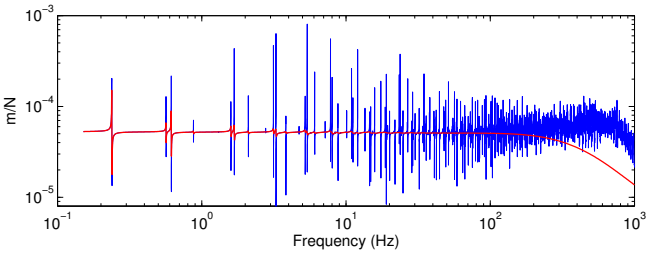

Fig. 5. Representative collocated transfer function for a force actuator, with (red line) and without (blue) active damping.

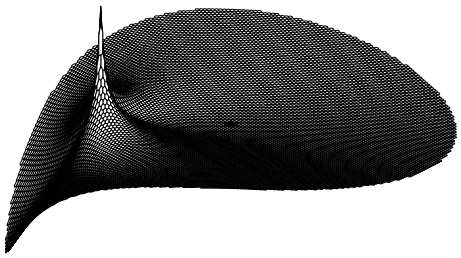

Fig. 6. Static response pattern for a torque command on a representative actuator (magnified); the influence pattern is non-local.

the correct set-point for each sensor; these techniques are well established on the ground but some modifications to the approach would be required to handle many thousands of segments [5]. Having mechanical edge sensors means that optical feedback is not continuously required, except for low-order mirror deformations that are not well observed by relative measurements between segments.

The transformation between segment motion and sensor response is known from geometry. The global piston, tip and tilt of the entire mirror cannot be measured with internal relative sensor measurements (nor controlled with relative actuators), aside from these degrees of freedom the transformation is invertible. For ground-based segmented-mirror arrays, the actuators influence the absolute motion of the segments, while the sensors measure relative motion, and for very large segment arrays, the transformation between the two would require both attention to robustness (which may be challenging to solve [12]) and to computation (which is straightforward to solve [13, 14]). Here the actuation only applies differential forces/torques between neighbouring segments, and so even if the sensors do not measure exactly the same degrees of freedom that the control algorithm uses, the transformation between the two can be local and robust. The control challenge in this application is managing the dynamics, rather than the static transformation between sensed and actuated degrees of freedom.

Some representative characteristics of the mirror are shown in Fig. 5 and 6, including the transfer function between a representative actuator and the collocated response, and the static response shape of the mirror resulting from a unit command on a representative actuator.

It is convenient to conceptually divide the control problem into two steps; adding active damping, and position feedback. There are two key requirements that must be demonstrated for control. First, the ability to add active damping despite

the need to eventually roll-off due to finite actuator/sensor dynamics (i.e. compensating for the behavior in Fig. 5). And second, the ability to manage the wide range of spatial scales introduced by actuation without requiring global knowledge that would inevitably limit robustness (i.e. compensating for the behavior in Fig. 6). Approaches for these key challenges are described in Sections IV-B and IV-C below.

B. Active damping

Collocated rate feedback can add significant damping, making the position control design more straightforward. While this is guaranteed to be robustly stable, in practice, rate feedback has finite bandwidth due to sensor and actuator dynamics and electronic implementation [15]. While the simulation here has a highest resonant frequency $\sim$1.5 kHz, the real mirror will have higher frequency resonances due to internal segment dynamics. With no natural damping, the active damping would require infinite bandwidth. In order to roll-off (intentionally or due to actuator/sensor dynamics), the negative compensator slope would result in phase that violated positive-real conditions for stability.

However, with non-zero natural damping, [10] illustrates that there will always be some frequency at which the half-power bandwidth of a resonant mode will exceed the modal spacing by a sufficient factor so that the transfer function above this frequency is relatively smooth in both magnitude and phase. This is sufficient to always allow active damping roll-off provided that the active damping has a minimum bandwidth. The high number of modes in this problem means that this "acoustic limit" for the structural behavior is at a low enough frequency that active damping is plausible with realistic actuator and sensor bandwidths.

The magnitude of the rate feedback for each actuator is chosen to give as much as 50% damping of higher-frequency structural modes; note that with a large number of collocated actuator/sensor pairs, then each actuator does not need to provide significant damping for the overall modes to have significant damping. A representative resulting transfer function is shown in Fig. 5, yielding a more straightforward problem for position control.

C. Local Position feedback

Collocated position feedback is guaranteed stable since the system is passive (this adds electronic stiffness), but with zero phase margin. Because roll-off is required at some frequency, the maximum stable gain does not yield a significant performance improvement over open-loop (loop gain less than unity at low frequency). Integral control would give zero steady-state error, but is not guaranteed to be stable; indeed it is straightforward to robustly close a single actuator/sensor loop with high-bandwidth integral control, but simultaneously closing all of the collocated actuator/sensor loops is unstable at small gain.

The reason for this is that, as evidenced by the static response pattern in Fig. 6, the control has much higher gain on low spatial-frequency deflection patterns than on high (that is, the plant is ill-conditioned). A collocated strategy means that in response to a particular non-zero inter-segment

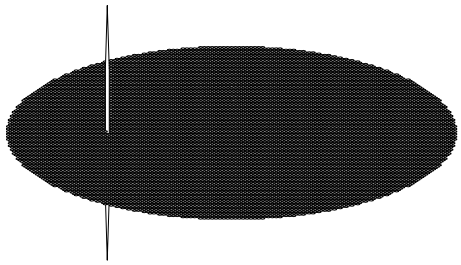

Fig. 7. Static response pattern for a command to a representative local family group in response to a single segment rotation error; compare with Fig. 6. The response away from the segment is negligible.

motion, the control will apply solely the corresponding relative actuator command, giving a global response to a local error. A global feedback strategy could readily avoid this, by inverting the system dynamics, at the expense of requiring, and hence being dependent on, both global model knowledge and global information. The innovation used herein is to use only local actuation in response to a particular segment displacement; this provides a remarkably good compromise between performance and required knowledge.

Define the set Ω_k of actuators local to segment k; here we use all actuators on both that segment and all adjacent segments for a total of 60 (out of 72 000) actuators for an interior segment.

The static response of the mirror to an actuator command is $x = C\Phi f$, where $C = K^{\#}$ is a modified compliance matrix, where the uncontrollable rigid body modes are projected out (C is the pseudo-inverse of K, note that eigenvectors corresponding to zero eigenvalues of K are also uncontrollable). C is fully-populated and ill-conditioned.

Define the state $x = e_{ki}$ to be a unit displacement of coordinate i on segment k, and choose the actuator response pattern f_{ki} that minimizes the cost function

$$J = \|C\Phi f_{ki} - e_{ki}\|_2 \tag{2}$$

subject to the constraint that elements of the vector f_{ki} not in the set Ω_k must be zero. That is, choose a local set of forces to minimize the error over the entire mirror in matching the displacement pattern. The constrained least-squares problem is equivalent to solving an unconstrained problem with a truncated matrix $\Psi_k = C\Phi_{:,\Omega_k}$, where only the columns of Φ associated with actuators in Ω_k are retained. The row of the pseudo-inverse of Ψ_k corresponding to the i^{th} coordinate on the k^{th} segment gives the appropriate local force distribution f_{ki} to compensate for an error at location k. Assembling, for each k and i, the resulting pattern into a matrix Q (so $Q_{\Omega_k,ki} = f_{ki}$), then Q gives an approximate inverse to the system at zero-frequency, based on local actuation only, and the control u based on Qx gives substantially better performance than collocated control. This approach is identical in derivation to that in [10], and motivated by the local approach used in [16] to develop computationally efficient sparse reconstructor matrices for adaptive optics estimation. The resulting response distribution to a single segment rotation error is shown in Fig. 7; the response to a position error is similarly local.

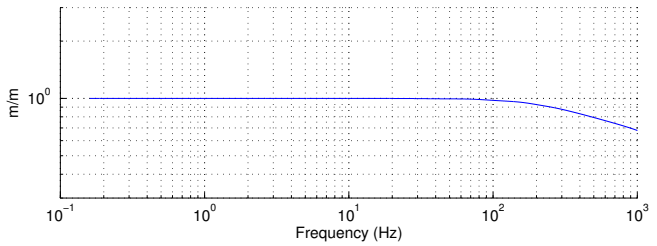

Fig. 8. Representative transfer function from an input to a local force distribution to the resulting segment position response. In addition to the modes of the system being well damped, the system dynamics are normalized so that the low- and high-spatial frequency gains are comparable.

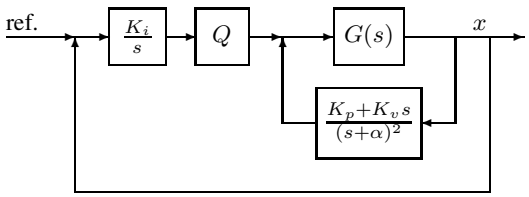

Fig. 9. Block diagram of control system. $G(s)$ is the open-loop system with 36 000 states and nearly 72 000 actuators. Rate feedback K_v adds damping, position gain K_p adds stiffness, but both are limited by actuator and sensor dynamics represented above by poles at $s = -\alpha$. The outer position control loop is made better conditioned using the matrix Q; this is sparse and local, and provides an approximate inverse to the static plant.

With this (static) transformation between segment position errors and the appropriate corresponding force distribution, it is much more straightforward to design a position controller. A representative transfer function between an input to a single local actuator group and the resulting segment response is shown in Fig. 8; since Q is an approximate static inverse of the plant, the resulting system is decoupled and normalized to unit gain at zero frequency. The block diagram for the resulting architecture is shown in Fig. 9.

V. DISCUSSION

Active control is an enabler for future space telescopes with primary mirror areal densities an order of magnitude smaller than current generation telescopes, permitting an order of magnitude greater collecting area for the same launch weight. Concepts for highly-segmented large aperture space telescopes have been presented before, however, there are several challenges that must be overcome before these can be seriously considered for future missions. One key issue is the ability to control the resulting segment array, requiring control of many degrees of freedom, with many lightly-damped structural modes within the control bandwidth. Building off of recent research in controlling large flexible deformable mirrors, a control architecture is presented here that combines active damping with local position control. There are two key challenges.

First, there are thousands of lightly-damped modes, yet any real actuators and sensors have finite bandwidth, and thus any implementation of rate feedback to add damping will not be positive real above some frequency. It is therefore essential to recognize that there will always be some frequency at which the structure enters an "acoustic limit", where the half-power bandwidth of any mode exceeds the modal spacing, and thus the phase excursions in the collocated transfer function decrease, due to multiple modes being simultaneously excited. It is precisely because there are many structural modes in this problem that this frequency is not unrealistically high, and hence practical active damping is stable provided it has a minimum bandwidth.

Second, in addition to the wide range of temporal frequencies, there is a wide range of spatial frequencies excited by any actuator, so that the response to an actuator command is global. Collocated position feedback thus suffers because a global response pattern is generated in response to a local position error. A global feedback strategy could certainly correct this behavior, but requiring information from the entire mirror has the potential to introduce robustness problems. Instead, we introduce a local control strategy that does not depend on model or state knowledge far away from a given actuator. In contrast to typical distributed control derivations, this is derived not by considering what nearby information is necessary at each actuator location, but what distribution of response is appropriate for any given local position error.

The strategy is demonstrated on a dynamic model of a 30 m mirror composed of 12 000 identical 30 cm diameter segments. The ability to control the system is not a barrier to designing a space telescope with a large number of segments!

REFERENCES

[1] M. Postman *et al.*, "Science drivers and requirements for an Advanced Technology Large Aperture Space Telescope (ATLAST): Implications for technology development and synergies with other future facilities," in *SPIE 7731, Space Telescopes and Instrumentation*, 2010.

[2] J. Nelson and G. H. Sanders, "The status of the Thirty Meter Telescope project," in *Ground-based and Airborne Telescopes II*, L. M. Stepp and R. Gilmozzi, Eds., vol. 7012. SPIE, 2008.

[3] R. Gilmozzi and J. Spyromilio, "The 42m European ELT: status," in *Ground-based and Airborne Telescopes II*, L. M. Stepp and R. Gilmozzi, Eds., vol. 7012. SPIE, 2008.

[4] J. P. Gardner *et al.*, "The James Webb Space Telescope," *Space Science Reviews*, vol. 123, pp. 485–606, 2006.

[5] D. C. Redding, G. S. Hickey, and S. C. Unwin, "Actuated mirrors for space telescopes," in *SPIE 7731*, 2010.

[6] R. G. Dekany, D. G. MacMartin, G. A. Chanan, and M. Troy, "Advanced segmented silicon space telescope (ASSiST)," in *SPIE 4849: Highly Innovative Space Telescope Concepts*, 2002.

[7] K. Patterson, S. Pellegrino, and J. Breckinridge, "Shape correction of thin mirrors in a reconfigurable modular space telescope," in *SPIE 7731, Space Telescopes and Instrumentation*, 2010.

[8] S. Padin, "Design considerations for a highly segmented mirror," *Applied Optics*, vol. 42, no. 16, pp. 3305–3312, 2003.

[9] M. J. Santer and K. A. Seffen, "Optical space telescope structures: The state of the art and future directions," *Aeronautical Journal*, vol. 113, no. 1148, pp. 633–645, 2009.

[10] D. G. MacMynowski, R. Heimsten, and T. Andersen, "Distributed force control of deformable mirrors," *European J. Control*, 2011.

[11] J. H. Burge, E. Sabatke, J. R. P. Angel, and N. J. Woolf, "Optical design of giant telescopes for space," in *SPIE 4092, Novel Optical Systems Design and Optimization III*, 2000.

[12] D. G. MacMynowski, "Interaction matrix uncertainty in active (and adaptive) optics," *Applied Optics*, vol. 48, no. 11, 2009.

[13] ——, "Hierarchic estimation for control of segmented-mirror telescopes," *AIAA J. Guid., Control & Dynamics*, vol. 28, no. 5, 2005.

[14] L. Lessard, M. West, D. MacMynowski, and S. Lall, "Warm-started wavefront reconstruction for adaptive optics," *J. Opt. Soc. Am. A*, vol. 25, no. 5, pp. 1147–1155, 2008.

[15] A. Preumont, *Vibration Control of Active Structures: An Introduction*. Kluwer Academic Publishers, 2002.

[16] D. G. MacMartin, "Local, hierarchic, and iterative reconstructors for adaptive optics," *J. Optical Society America, A*, vol. 20, no. 6, 2003.